Mechanisms of Tissue Uptake and Retention in Zotarolimus-Coated Balloon Therapy

Citation: Kolachalama, V. B., S. D. Pacetti, J. W. Franses, J. J. Stankus, H. Q. Zhao, T. Shazly, A. Nikanorov, L. B. Schwartz, A. R. Tzafriri, and E. R. Edelman. "Mechanisms of Tissue Uptake and Retention in Zotarolimus-Coated Balloon Therapy." Circulation 127, no. 20 (April 12, 2013): 2047–2055.

As Published: http://dx.doi.org/10.1161/circulationaha.113.002051

Publisher: American Heart Association

Persistent URL: http://hdl.handle.net/1721.1/102576

Version: Author's final manuscript: final author's manuscript post peer review, without publisher's formatting or copy editing

Published in final edited form as:
Circulation. 2013 May 21; 127(20): 2047–2055. doi:10.1161/CIRCULATIONAHA.113.002051.

Mechanisms of Tissue Uptake and Retention in Zotarolimus-Coated Balloon Therapy

Vijaya B. Kolachalama, PhD[1,2], **Stephen D. Pacetti, MS**[3], **Joseph W. Franses, PhD**[1], **John J. Stankus, PhD**[3], **Hugh Q. Zhao, PhD**[3], **Tarek Shazly, PhD**[1,4], **Alexander Nikanorov, MD, PhD**[3], **Lewis B. Schwartz, MD**[3], **Abraham R. Tzafriri, PhD**[1,5], and **Elazer R. Edelman, MD, PhD**[1,6]

[1]Harvard–MIT Division of Health Sciences and Technology, Cambridge, MA

[2]Charles Stark Draper Laboratory, Cambridge, MA

[3]Abbott Vascular, Santa Clara, CA

[4]University of South Carolina, Columbia, SC

[5]CBSET Inc., Lexington, MA

[6]Brigham and Women's Hospital, Boston, MA

Abstract

Background—Drug-coated balloons are increasingly utilized for peripheral vascular disease and yet, mechanisms of tissue uptake and retention remain poorly characterized. Most systems to date have used Paclitaxel, touting its propensity to associate with various excipients that can optimize its transfer and retention. We examined Zotarolimus pharmacokinetics.

Methods and results—Animal studies, bench-top experiments and computational modeling were integrated to quantify arterial distribution after Zotarolimus-coated balloon (ZCB) use. Drug diffusivity and binding parameters for use in computational modeling were estimated from kinetics of Zotarolimus uptake into excised porcine femoral artery specimens immersed in radiolabeled drug solutions. Like Paclitaxel, Zotarolimus exhibited high partitioning into the arterial wall. Exposure of intimal tissue to drug revealed differential distribution patterns, with Zotarolimus concentration decreasing with transmural depth as opposed to multiple peaks displayed by Paclitaxel. Drug release kinetics was measured by inflating ZCBs in whole blood. *In vivo* drug uptake in swine arteries increased with inflation time but not with balloon size. Simulations coupling transmural diffusion and reversible binding to tissue proteins predicted arterial distribution that correlated with *in vivo* uptake. Diffusion governed drug distribution soon after balloon expansion but binding determined drug retention.

Conclusions—Large bolus of Zotarolimus releases during balloon inflation, some of which pervades the tissue and a fraction of the remaining drug adheres to the tissue-lumen interface. As a result, duration of delivery modulates tissue uptake where diffusion and reversible binding to tissue proteins determine drug transport and retention, respectively.

Correspondence: Vijaya B. Kolachalama, PhD, 555 Technology Square, Cambridge, MA – 02139, Phone: 617-258-4718, Fax: 617-258-3927, vkolachalama@draper.com.

Author contributions: Conception, design and study direction: VBK, SDP, AN, LBS and ERE. Bench-top and animal studies: VBK, SDP, JWF, JJS, HQZ and TS. Computational modeling: VBK, TS and ART. Data analysis: VBK, SDP, JWF, ART and ERE. Manuscript write-up: VBK, SDP, ART and ERE.

Conflict of Interest Disclosures: None.

Keywords

Drug-coated balloon; Zotarolimus; Peripheral vascular disease; Computational modeling; Animal model

Introduction

Peripheral artery disease remains a clinical challenge despite advances in angioplasty and stenting.[1, 2] Intervention using drug-coated balloons (DCBs) is emerging as a potentially viable strategy,[3] demonstrating clinical efficacy at inhibiting restenosis following angioplasty in the lower extremities.[4, 5] Use of DCBs can open occluded vessels and concomitantly deliver drug to target lesions while avoiding the risks of chronic inflammation and incomplete healing associated with permanent implants such as stents. Most studies to date using DCBs have utilized Paclitaxel, with a range of hydrophilic carriers and coatings, and have demonstrated varying levels of efficacy.[4–7] Recently, Zotarolimus-coated balloons (ZCBs) have shown efficacy within hypercholesterolemic femoral arteries in swine.[8] While positive results have been observed in peripheral applications, use of DCBs in *de novo* or STEMI coronary lesions in conjunction with a BMS has shown a lack of efficacy versus a conventional drug-eluting stent (DES).[9, 10] Safety concerns raised by these data illustrate a need for better understanding of drug distribution and residence time. Debate continues as to whether DCBs induce sustained, desirable clinical effects and if bolus release of drug at the lumen-tissue (or mural) interface during balloon expansion is a clinically efficacious mode of delivery.

We sought to determine the mechanisms that govern arterial uptake and distribution of balloon delivered drugs with a focus on Zotarolimus. Using an integrative framework coupling *in vivo*, bench-top and computational models of ZCBs deployed in porcine arteries, we quantified spatio-temporal arterial drug distribution patterns. Tissue incubation experiments using radiolabeled Zotarolimus and Paclitaxel provided estimates of the partition constants, tissue binding capacities and transmural drug diffusivities, with Paclitaxel serving as a benchmark during experimental determination of the transport constants. *In vitro* release experiments of ZCBs expanded for different durations in porcine blood estimated the amount of releasable drug that is transferred to the tissue during balloon expansion. *In vivo* studies using ZCBs exposed for two inflation times revealed a dependence of tissue content with delivery duration. Simulations performed on a computational model constructed using the bench-top parameter estimates revealed that time varying arterial drug distribution patterns resulting from balloon delivery are governed by a delicate balance between diffusion mediated drug transport into the arterial wall and reversible binding to tissue ultrastructural elements.

Materials and methods

Net partition constant and binding parameters

Arterial partition constants of Zotarolimus and Paclitaxel dissolved in phosphate buffered saline (PBS) were measured. Unlabeled and radiolabeled analogs of each drug were mixed at a ratio of 100:1 as this provided sufficient signal for measuring tissue concentrations via liquid scintillation counting. Drug bath solutions were prepared at 5, 10, and 20 μM concentrations in PBS (pH~7.4) containing 4% (w/v) bovine serum albumin (BSA) and stored in glass vials at 4°C. 2% PEG-200 (w/w) was added to all solutions to improve aqueous solubility of the drugs and prevent nonspecific adhesion to glass.[11] Unlabeled and radiolabeled Zotarolimus ([^{3}H]-Zot) were donated by Abbott Vascular (Santa Clara, CA) and Abbott Laboratories (Abbott Park, IL), respectively. Unlabeled Paclitaxel was

purchased from LC Laboratories (Woburn, MA), and radiolabeled Paclitaxel ([^{3}H]-Pxl) from ViTrax (Placentia, CA). Porcine femoral arteries, immersed immediately in a 4°C bath of PBS (pH ~7.4) containing 4% BSA, were obtained from a local slaughterhouse within hours of sacrifice (Research 87, Boylston, MA). Arteries were cleaned of excess fascia, cut into small cross-sectional segments (20–60 mg), and placed in glass vials with drug bath solutions at 4°C for different incubation times up to 96 hrs. All samples were placed on a shaker at 10–20 rpm to homogenize the drug bath and facilitate uniform exposure to tissue. After incubation, each tissue sample was immersed in a separate glass vial containing 1 mL of an aqueous solubilizer (Solvable™, PerkinElmer Inc.) and dissolved at 55°C with shaking for 24 hrs. 200 μL of the dissolved liquid from each vial processed in triplicate was combined with a pseudocumene-based cocktail (Hionic-Fluor, PerkinElmer Inc.) for liquid scintillation counting. The net partition constant (κ) was then defined as the ratio of the relative vial concentration of the digested tissue sample appropriately normalized with tissue sample weight (C_T in μM) and the drug bath concentration (C_{bulk} in μM).

Net tissue binding capacity (B_M in μM) and equilibrium dissociation constant (K_d in μM) were estimated by varying the concentration of drug solutions (5–20 μM) and considering the variations in κ for 96 hrs. Experimental partition constant values were then fit (GraphPad Prism 3.0) to the relationship implied by bimolecular binding of small hydrophobic drugs that have access to the entire tissue volume[12]:

$$\kappa = 1 + \frac{B_M}{(K_d + C_{\text{bulk}})}. \quad (1)$$

Transmural distribution and effective diffusion coefficient

Intra arterial distributions of Zotarolimus and Paclitaxel were measured using a diffusion chamber (Harvard Apparatus) (Figure 1A). To minimize hydrophobic drug binding to the interior walls of the diffusion chamber, hydrophilic surface modification was performed by incubating the chamber in 10 μM poly(L-lysine) for 6 hrs at room temperature. Porcine femoral arteries prepared as described above were cut into small segments (~2×2 cm^2) and affixed between the opposing faces of the wells within the diffusion chamber using a series of pins surrounding the opening. The half chambers were comprised of baths containing 10 μM of drug dissolved in PBS + 4% BSA + 2% PEG-200; drug free baths were used as controls. Tissue samples were maintained at a steady bath concentration gradient for 1 hr at room temperature. Magnetic stir bars were used throughout the incubation to ensure adequate bath homogeneity. After incubation, samples were snap frozen with liquid nitrogen cooled isopentane and immediately stored at −80°C until further analysis.

The mass of each frozen segment was recorded and 20 μm sections were cut parallel to the intima with a cryotome (Leica Inc.). Triplets of consecutive sections were placed together in a glass vial containing 1 mL of Solvable™ and subsequently digested at 55°C for 24 hrs. Liquid scintillation counting was used to measure drug concentration in each vial containing dissolved tissue and Hionic-Fluor. Net tissue concentration in each vial was then normalized to the highest estimated mean concentration from all the vials and plotted using midpoint of each triplet of sections as the transmural location on the abscissa (Figure 2B). For each distribution profile, permeation depth (L_P), denoted as the distance at which the ratio of intra arterial tissue and the source concentrations at the mural surface reaches 0.083 (see Supplement) was calculated and the effective diffusivity (D_{eff}) of the total drug within tissue was estimated from the equation:

$$D_{\text{eff}}=\frac{L_p^2}{6t} \quad (2)$$

where t is the total time of incubation.[13] D_{eff} represents apparent net diffusivity of free and bound drug within the arterial tissue, which is lower than diffusivity in fluid due to the combined effects of steric hindrance and reversible binding to immobilized proteins. As tissues were exposed to low drug concentrations, the diffusivity of free drug (D_T) was estimated using the result for unsaturated drug binding (see Supplement):

$$D_T=\left(1+\frac{B_M}{K_d}\right)D_{\text{eff}}. \quad (3)$$

Transfer kinetics

The amount of releasable Zotarolimus during balloon expansion was measured with ZCBs (6×40 mm, dose: 300 μg/cm^2; Figure 1B), in a bench-top system. A 250 mL beaker filled with citrated porcine blood, gently stirred, and maintained at 37°C was used to maintain sink conditions. A fresh aliquot of blood was used for each balloon. A ZCB was placed into the solution, inflated to 2 atm and was held in solution for the designated time. The balloon was immediately removed, followed by release of pressure on the balloon and excision of the balloon from the catheter. Extracted balloons were then placed in individual vials and rapidly frozen at −20°C. Experiments were performed in triplicate at four different expansion times (30–300 s) along with a control arm of zero expansion time. For all balloons, drug content was quantified via HPLC after extraction (column: Zorbax Eclipse XDB-C18, 3.5 μm, 4.6×50 mm; temperature: 60°C; flow rate: 1.2 mL/min; mobile phase: 10 mM ammonium acetate buffer/acetonitrile gradient; injection volume: 10 μL; detection: A_{277}). Drug released was calculated as the difference relative to ontrol ZCBs. Amount of Zotarolimus released from balloons was normalized to the area of the balloon to obtain the flux (J_b) which was fit to one phase exponential association kinetics as follows:

$$J_b(t)=A_1\left(1-e^{-k_1 t}\right). \quad (4)$$

Here, t is the time and A_1 and k_1 are empirically estimated using curve fitting (GraphPad Prism 3.0).

In vivo tissue uptake

Tissue uptake and retention of Zotarolimus was estimated in domestic farm swine of either gender (30±5 kg, n = 18). All animals received standard care in accordance with the Animal Welfare Act and the “Principles of Care of Laboratory Animals” formulated by the Institute of Laboratory Animal Resources (National Research Council, NIH publication No.85–23, revised 1996). Clopidogrel (150 mg) and Aspirin (325 mg), and Enrofloxacin (5 mg/kg) were administered one day before and on the day of the procedure. Nifedipine (30 mg) was provided one day before the procedure in the evening and on the day of the procedure in the morning. Buprenorphine at (0.01–0.06 mg/kg) was administered as needed for pain management. 8Fr femoral or iliac arterial access was obtained. Following heparinization, each animal was treated with four balloons in the external iliac and the superficial femoral arteries (SFA) and/or profunda arteries (Figure S1, Supplement). The balloon coating comprised of Zotarolimus combined with proprietary excipients at a weight fraction of ~0.59. The exact location of the treatment site of the artery was identified based on

angiograms using anatomic landmarks as references and a scaling factor calculated based on actual and measured balloon length.

Arteries were exposed to 30±1 s or 180±2 s inflations (Figure S1, Supplement). Fox sv PTA catheters (Abbott Vascular, CA) with drug dose (300 μg/cm^2) available in two sizes 5×40 mm (1.88 mg/balloon) and 6×40 mm (2.26 mg/balloon) were used to enable appropriate sizing and target balloon-artery expansion ratio (1.2:1). Overall mean swine arterial diameter in the study was 4.8±0.6 mm. 200 μg of Nitroglycerin was administered intraluminally as needed to control arterial vasospasm. Animals were euthanized after 5 min, 4 hrs and 24 hrs, treated arteries were excised and collected based on angiography data using anatomic landmarks as references. At the end of respective time points, vessels from each animal were dissected out in the same order as that of the treatment, and the arteries were carefully cleaned from surrounding connective tissue. Cleaned arteries were placed in glass vials that were snap frozen in liquid nitrogen and stored at −80°C. For analysis of the Zotarolimus content, each arterial tissue specimen was thawed, weighed and processed for assaying by liquid chromatography coupled with mass spectroscopic detection (LC-MS).[14]

Computational model

Transient drug distribution from an expanded DCB was modeled as a two dimensional continuum transport problem. The computational domain comprised of an arterial cross-section with radius (R = 3 mm) and wall thickness (T = 0.5 mm) (Figure 1C). Free drug was allowed to diffuse with a constant diffusivity (D_T) and reversibly bind to nonspecific tissue sites according to the local balance equations:[12]

$$\frac{\partial C_f}{\partial t}=D_T\nabla^2 C_f-\frac{\partial B}{\partial t} \quad (5)$$

and

$$\frac{\partial B}{\partial t}=k_a C_f(B_M-B)-k_d B. \quad (6)$$

The variables C_f and B denote the local concentrations of free and bound drug in the arterial wall, respectively, B_M is the net tissue binding capacity and, k_a and k_d are the association and dissociation rate constants, respectively. The above equations were solved subject to zero initial free and bound drug concentrations within the tissue, flux boundary condition during balloon inflation at the mural surface and perfect sink condition at the adventitial surface. At the mural surface, drug influx is prescribed as:

$$J_s(t)=\begin{cases} J_b(t), & t \le t_0 \\ 0, & t>t_0 \end{cases} \quad (7)$$

where t_0 is the balloon inflation time and $J_b(t)$ (mol/m^2.s) is the flux approximating the releasable portion of Zotarolimus from the balloon during inflation (Equation 4). Once the balloon has been deflated and retracted, bulk transferred drug at the mural surface becomes exposed to flowing blood and can be cleared depending on its adherence to the wall and solubility in blood. Rather than modeling adherence and solubilization, we considered two opposing extremes; either that mural adhered drug is insensitive to flowing blood, modeled as zero flux condition on this interface (Equation 7) or that blood is extremely efficient at clearing mural adhered drug, modeled as a zero concentration condition:

$$J_s(t)=J_b(t),\ t \leq t_0 \text{ and } C_s(t)=0,\ t>t_0. \quad (8)$$

Constants including B_M, K_d, and D_T were estimated from the bench-top experiments. k_a and k_d were then computed as $k_a=\frac{D_T D_a}{B_M T^2}$ and $k_d = k_a K_d$. Here, D_a = 50,000 is the Damkohler number based on Rapamycin data.[5] Time dependent simulations (COMSOL Inc.) were performed on the computational domain that was meshed using the Delaunay triangulation scheme. A zero concentration condition was applied on the perivascular side of the arterial wall for the free drug. For the bound drug, both the intramural and the perivascular aspects of the arterial wall were assigned a zero flux boundary condition. The Direct (SPOOLES) method was used to solve the system of equations with a nested dissection pre-ordering algorithm and a backward differentiation formula method was used for time integration with relative and absolute tolerances for the time stepping assigned at 10^{-6} and 10^{-8}, respectively. Simulations were performed until the Newton iterations of the fully coupled solver reached 1,000 or when the minimum damping and tolerance factors reached 10^{-4} and 1, respectively. The methodology was deemed mesh independent when there was <2% difference in the mean free drug concentration within the arterial wall for successive mesh refinements, and the resultant mesh comprising 21,208 triangular elements was used for all subsequent simulations.

Statistical analysis

Experimental data are expressed as mean±SEM. For transmural distribution data (Figure 2B), an F-test was performed to determine the goodness of fit of the linear distribution. When sample normality was justified, statistical comparisons between groups were performed with the unpaired student t-test assuming unequal variances. When normality could not be supported, the two-sample Mann–Whitney test was used. The p-values presented were derived from the t-test unless otherwise indicated. Experimental differences were statistically significant at $p < 0.05$.

Results

Arterial uptake of Zotarolimus and Paclitaxel greatly exceeded the applied bulk concentrations (Figure 2A), as reflected by their large partition constants ($\kappa \gg 1$). Bath concentrations (5, 10 and 20 μM) were selected to simulate high concentration source conditions. Estimated net partition constants increased initially with time and approached steady state. For example, partition constant for Zotarolimus increased ~1.5-fold from 24 to 69 hrs and remaining relatively unchanged with further increase in time. Based on these observations, a bath concentration of 10 μM and an incubation time of 69 hrs were chosen for subsequent experiments to simulate saturating drug conditions. Curve fitting (Equation 1) on the distribution profiles of both drugs estimated κ under these conditions (9.3±0.4 for Zotarolimus and 9.4±0.8 for Paclitaxel) and provided estimates of the equilibrium binding parameters (B_M = 0.356 mM and K_d = 0.0326 mM, R^2 = 0.999) for Zotarolimus and (B_M = 1.3 mM and K_d = 0.136 mM, R^2 = 0.515) for Paclitaxel.

When drugs were exposed to the luminal side of the artery affixed within the diffusion chamber, Zotarolimus uptake was maximal within the intimal region and decreased linearly with increasing distance from the intraluminal side (Figure 2B, linear regression and F-test: $p < 0.00005$). In contrast, Paclitaxel uptake displayed multiple peaks across the arterial wall (Figure 2B, linear regression and F-test: $p > 0.05$). While Zotarolimus uptake was over 13-fold higher at the intima as compared to the uptake within the last transmurally grouped layer of the adventitia, Paclitaxel uptake was only ~3-fold higher. Estimated apparent net

diffusivity (D_{eff}) of Paclitaxel (54.1±34.3 $\mu m^2/s$) was over 3-fold higher than that of Zotarolimus (17.1±5.1 $\mu m^2/s$). The true diffusivity (D_T) for unbound (free) Zotarolimus within the tissue then becomes 204.1 $\mu m^2/s$ (Equation 3).

Only ~2% of total drug on the coating and ~24% of the releasable drug is transferred during 30 s inflation time (Figure 3A). Release followed first order kinetics with a half life of ~75 s, where drug release from the balloon rapidly increased after balloon expansion and reached steady state within ~5 min. This profile may reflect a solubilizing effect of a finite amount of excipient, which is subsequently depleted, or it may be attributed to the progressive smoothing of initially porous, high surface area morphology, slowing the release. In the presence of a monolithic, phase separated coating, rapid release may reflect diffusion of a small amount of percolating drug on the surface of the balloon. Slower release afterwards denotes the absence of sufficient time to allow remaining drug to solubilize and diffuse through the coating.[15] Micrographs of treated arteries illustrate that some Zotarolimus released during balloon expansion adheres directly to the mural surface and creates a thin layer of drug coating (Figure 3B). Our data speak to bulk transfer of drug from the expanded balloon onto the mural surface followed by transport via diffusion and reversible binding within the arterial wall. Total drug uptake averaged over the treated tissue displayed bi-phasic kinetics, with an initial first order decline phase during the first 4 hrs that was succeeded by slower efflux of drug (Figures 4A & 4B). About 98% of Zotarolimus taken up by the artery was cleared between 5 min and 24 hrs after 30 s balloon inflation. Yet, resulting arterial levels at 24 hrs reflect detectable and potentially therapeutic levels of Zotarolimus (1.4±0.5 ng/mg). Arteries exposed to 180 s balloon inflation exhibited higher tissue uptake than with 30 s exposure (Figures 4A & 4B) for SFA and iliac arteries (Table S1, Supplement), and tissue uptake was independent of balloon size (Table S2, Supplement). Tissue uptake in profunda arteries at 4 hrs was ~7-fold ($p < 0.01$) and ~8-fold ($p < 0.01$) higher than the SFA and iliac arteries for 30 s and 180 s balloon exposure times, respectively. Duration of balloon exposure to arteries impacted uptake in profunda arteries as well with 97% higher uptake observed at 4 hrs ($p < 0.02$), when inflation time rose 6-fold to 180 from 30 s. Model simulations based on the bench-top estimated binding parameters also predicted bi-phasic kinetics for total drug (Figures 4A & 4B) as well as the unbound and bound drug concentrations (Figure 5A), and the predicted free to bound drug ratio becomes ~9:10 and ~1:1 after exposure to 30 s and 180 s balloon inflations, respectively. This ratio increased exponentially in the first hour post expansion and reached a steady state within the next few hours (Figure 5B). Simulations that varied only the drug diffusivity relative to *in vitro* estimates resulted in an envelope of distribution profiles with a trend similar to that of the *in vivo* measurements. For both inflation durations (Figures 4A & 4B), *in vivo* tissue uptake is consistent with the assumption that the thin layer of adhered drug that is left behind post balloon retraction shields sub-intimal drug from clearance by flowing blood (Equation 7). Contrastingly, simulations that assumed a highly permeable layer of mural adhered drug that allows for efficient washout of sub-intimal drug underestimated the *in vivo* trend line (Figures S2 & S3, Supplement). Having demonstrated the correlation between computationally modeled and *in vivo* derived tissue content, we examined model based predictions of the dynamics of arterial drug distribution. Simulations illustrate that mural drug transfer within the short inflation time (30 s) gives rise to a penetration front of drug up to ~130 μm into the arterial wall (Figure 6A). Concomitantly, binding sites are fully saturated up to a depth of ~70 μm, although the majority of distributed drug is unbound up to a depth of ~40 μm (Figure 6B). By 5 min, drug has already permeated throughout the arterial wall (Figure 6C) and as only free drug can diffuse and be cleared from the artery, Zotarolimus is predicted to be mostly bound by 5 min (Figure 6D). These simulations demonstrate that diffusion quickly and efficiently distributes Zotarolimus throughout the arterial wall and that drug binding to ultrastructural elements can explain observed *in vivo* retention kinetics in DCB-treated arteries. Simulations predicted the same qualitative

distribution patterns when arteries were exposed to 180 s balloon inflation (Figure S4, Supplement).

Penetration depth was estimated at ~350 μm with drug predominantly present in the unbound form near the intima whereas saturation of binding sites within the medial region allowed Zotarolimus to reside in the bound state at the end of balloon inflation. By 5 min, Zotarolimus distributed across the arterial wall with drug predominantly bound to tissue proteins, where free to bound drug ratio decreased with transmural depth. Taken together, these results corroborate recent reports of ZCB efficacy in porcine arteries and the potential for Zotarolimus in DCB therapy.

Discussion

Treatment of obstructive arterial disease using permanent endovascular implants is highly appealing. Yet, late in-stent thrombosis with drug-eluting devices and restenosis of their bare metal counterparts raise questions about long term safety and may temper enthusiasm for these modalities. DCB technologies might provide for efficient arterial delivery of critical compounds without permanent implants.[16] Emerging studies of long term DCB efficacy for coronary[6, 17] and peripheral[8] vascular beds focused on characterizing dose dependent biologic and vascular bed associated clinical responses. Preclinical and clinical results have been equivocal and it has been hypothesized that the ability to formulate suitable carriers for Paclitaxel makes it preferable for DCB delivery. Sirolimus and its derivatives have not been extensively studied and may not be similarly suited for achieving desirable clinical efficacy, and thereby leaving the community with just one alternative and fixed thrombotic potential. By coupling computational, bench-top and animal models, we generated an integrative framework by which to quantify the mechanisms of ZCB therapy for endovascular applications and examine whether known mechanisms of drug transport and binding can explain *in vivo* tissue content and retention.

Factors governing drug uptake and retention

Drug potency is not the sole determinant of the expected biological and ultimate clinical outcome following local delivery. Factors such as drug distribution and retention in and around target tissue become immensely important,[18] and it is incumbent upon us to understand their determinants. Our data illustrate the role of drug and tissue properties, duration of delivery, diffusion and binding in determining Zotarolimus uptake and retention in the underlying tissue.

Coating composition—DCB coatings are typically drug rich and incorporate low molecular weight excipients aimed to facilitate drug release and transfer to the vessel wall. Vessel-balloon contact times are short and the nature of contact during expansion and retraction as well as methods to modify coating composition to optimize balloon transferred drug are still being defined. Thus, mechanisms governing drug transfer to the wall, distribution therein and sustained retention have yet to be fully understood. This has led to competing mechanistic hypotheses as to the determinants of arterial distribution in DCB-treated arteries. Some argue that these processes are governed by transport and binding of soluble drug in the tissue,[17] and as such tissue distribution and retention within the arterial wall are governed by diffusion and binding of soluble drug, respectively. Others claim that a significant fraction of the transferred drug and excipients distribute in the artery in micro particulate form and that solubilization of these micro depots determines tissue retention.[17] From this perspective, the nature of the coating determines the amount of drug that adheres to the mural surface and the degree to which sub-intimal soluble drug is protected by the

mural adhered coating from clearance by flowing blood. Our computational model validates a process that integrates these elements.

Duration of delivery—Our *in vivo* results indicate that increasing arterial exposure time to an inflated balloon increased tissue uptake of Zotarolimus. These observations are consistent with a first order dependence of drug uptake on the duration of balloon inflation (Figure 3A) and the findings validated by computational simulations of Zotarolimus arterial distribution (Figures 4A & 4B). While prolonged balloon inflation might induce ischemia and arterial injury, the correlation between *in vivo* uptake data and the inflation time suggests the possibility of an optimal exposure time for ZCB-treated arteries. Penetration depth increased with balloon exposure time and drug was predominantly unbound at the end of respective inflation times. Shortly after balloon inflation, Zotarolimus permeated efficiently throughout the arterial wall irrespective of exposure time. These results indicate that longer balloon exposure leads to increased tissue uptake where diffusion and reversible binding to tissue proteins explain observed *in vivo* retention kinetics in ZCB-treated arteries.

Drug dependence—When arteries were exposed to a constant source of drug in a diffusion chamber, transmural distribution of Zotarolimus was maximal in the intima and consistently declined at increasing depths (Figure 2B). Such distribution is consistent with diffusion mediated transport and a relatively uniform distribution of drug binding sites across the artery wall. Contrastingly, under similar exposure, Paclitaxel distribution displayed multiple peaks within the intimal and medial regions (Figure 2B).[13, 19] Indeed, the multi-laminate structure of the arterial wall comprising elastin within the intimal and medial regions exhibits preferential binding to Paclitaxel and this phenomenon may partially explain its nonlinear distribution.[20] Thus, though both these potent anti proliferative agents are small and hydrophobic, our data speak to their differential interactions with tissue proteins and consistent with our previous finding for Paclitaxel and Sirolimus in calf carotid arteries.[19, 21] As binding determines drug retention, our results suggest that Paclitaxel and Zotarolimus may also be differentially retained in arterial tissue. Sensitivity analysis showed that increasing effective diffusivity does not necessarily imply higher tissue uptake (Figures 4A & 4B; Figures S2 & S3, Supplement). Higher diffusivity leads to faster transport and clearance that in turn places a threshold on tissue uptake by limiting drug availability for binding. Thus, parameters defining an efficient DCB delivery are bounded by a need for delivering large amount of drug within a short period and the rate by which binding determines tissue retention.

Early dominance of diffusion and the role of binding—Following balloon transfer of drug to the mural surface, Zotarolimus permeates the entire tissue within a short period (Figure 6C) via diffusion. High values of diffusivity and the resulting penetration depth of Zotarolimus ensure adequate and rapid arterial uptake during balloon expansion (Figures 6A & 6B) but also mediate faster drug clearance from the adventitial surface after balloon deflation. Consequently, greater arterial uptake comes at a cost of faster diffusive clearance, suggesting that drug diffusivity may be amenable to optimization. This might be achieved through manipulation of the size or charge of the drug[22] or through the choice of excipients or carriers that are added to the coating. This dual role of diffusion points to its dominating effect soon after balloon expansion as the drug within the arterial wall reaches a balanced state with perhaps seemingly adequate levels of concentration.

Binding plays a critical role in DCB therapy by protecting the drug from pervading out of the arterial wall. Our model results indicate that binding occurs immediately after drug exposure to tissue and Zotarolimus is mostly bound within 5 min of balloon expansion (Figures 6C & 6D). The ratio of bound to unbound Zotarolimus over time rises and reaches a steady state value within 4 hrs (Figure 4C) suggesting that binding determines long term

tissue concentration and retention. Consequently, strategies for increasing drug affinity to tissue proteins have the potential to significantly increase retention as factors including drug's binding potential and diffusivity modulate the balance between free and bound drug within the tissue.

Tissue dependence—The roles of binding and diffusion introduce a dependence on tissue that can limit the extrapolation of clinical and preclinical experiences between vascular beds. Each arterial bed differs in form and element as muscular and elastic arteries are different from each other. Individual tissue layers within these vascular beds may allow isotropic diffusion, however transport becomes anisotropic between alternating tissue layers of varying permeability. Certain arteries are anatomically structured to divide into several side branches, and as a result, area of the mural surface exposed to the inflated balloon is reduced. Such differences affect diffusion and our results point to a similar phenomenon. Specifically, profunda arteries retained significantly more drug at 4 hrs than SFA and iliac arteries. This difference might reflect differential permeability or binding capacity due to ultrastructural differences, or differences in adventitial washout due to the embedding of profunda arteries within dense muscle tissue. It may also reflect the inherent non-bifurcating nature of the profunda artery where a larger surface area is covered by the expanded balloon without drug loss into the side branches.

Arterial wall composition—Atherosclerotic vessels are composed of non-uniform layers of lipid, calcification and other inflammatory agents that create a heterogeneous wall ultrastructure. Balloon expansion within these vessels likely has differential effects that reflect different morphologies and compositions of the target tissue. Kinetics of drug transfer within a localized region of injury may be altered and these changes can lead to non-uniformities in drug distribution.[11, 23] Increasingly sophisticated disease animal models are being presented and yet the variability along each arterial segment, vascular bed and animal currently challenges the correlations we seek, especially as we focus on quantifying micro level tissue drug distribution. Nonetheless, we have previously observed that net tissue uptake into atheromatous rabbit arteries can mask significant differences in the tissue distribution patterns of Paclitaxel and Sirolimus derivatives.[11] Thus, the overall correlation between the *in vivo* tissue content and the computational model based predictions may very well carry into diseased animal and human arteries. Future studies should examine the correlations between models and *in vivo* data on a microscopic level where variations in tissue morphology are apparent in a given specimen and from one vessel to the other.

Study limitations and future directions

An integrative approach coupling *in vivo*, computational and bench-top models allowed us to understand the mechanisms governing Zotarolimus transfer from coated endovascular balloons and subsequent arterial distribution and retention. A two dimensional computational model provided estimates of drug retention and binding at different time points. This model allowed empiric estimation of drug transport within tissue and simulation of complex phenomenon of reversible binding within the arterial wall. However, assumptions were made to simplify our understanding and create a coherent connection between bench-top derived pharmacologic constants that were fed into the computational model and the model based predictions that matched with the *in vivo* data. For example, two sets of boundary conditions approximated two opposing scenarios - how flowing blood completely washes out the mural adhered drug and the case when the adhered drug is insensitive to flow. Future studies will be performed using higher fidelity models utilizing physiologically realistic geometries, anatomically meaningful arterial wall composition, and the rate at which mural adhered drug is cleared by systematically accounting the role of luminal flow.[24, 25]

Our bench-top, animal and computational models do not account for the presence of atherosclerotic plaque and calcification. Compositional changes in the artery that accompany increased atherosclerosis affect local tissue capacity for drug absorption and retention. As disease induced changes alter the distribution of drug binding proteins and interstitial lipid alters drug distribution, one might observe differences in healthy versus normal arteries and hence, tissue saturation of drug might be comparative but not similar. Moreover, it has been shown that Sirolimus derivatives are relatively less sensitive to lesion complexity than Paclitaxel,[11] suggesting that mechanisms of ZCB therapy explained in this study may remain intact as well for diseased vessels.

Conclusions

Drug-coated balloons can deliver to and sustain drug within the arterial wall but in a manner distinct from permanent implants such as drug-eluting stents. Large bolus of drug released from an endovascular balloon over a limited time adheres to the mural interface, some of which diffuses into the tissue and saturates the tissue binding sites up to a well defined penetration front. A delicate balance between diffusion, binding and clearance at the mural and adventitial interfaces determines subsequent distribution and retention. This balance depends on the duration of delivery, the degree to which the adherent layer of mural drug shields sub-intimal soluble drug from blood washout, the binding capacity of the arterial bed and is amenable to optimization via manipulation of drug diffusivity and nonspecific binding properties.

Supplementary Material

Refer to Web version on PubMed Central for supplementary material.

Acknowledgments

Funding Sources: This study was supported in part by NIH grant (R01 GM-49039) to ERE and Abbott Vascular, Santa Clara, CA.

References

1. Finn AV, Nakazawa G, Virmani R. Pathology of drug-eluting stents: implications for coronary intervention. Indian Heart J. 2007; 59:B41–49. [PubMed: 19153436]
2. Joner M, Finn AV, Farb A, Mont EK, Kolodgie FD, Ladich E, Kutys R, Skorija K, Gold HK, Virmani R. Pathology of drug-eluting stents in humans: delayed healing and late thrombotic risk. J Am Coll Cardiol. 2006; 48:193–202. [PubMed: 16814667]
3. Gray WA, Granada JF. Drug-coated balloons for the prevention of vascular restenosis. Circulation. 2010; 121:2672–2680. [PubMed: 20566965]
4. Tepe G, Zeller T, Albrecht T, Heller S, Schwarzwalder U, Beregi JP, Claussen CD, Oldenburg A, Scheller B, Speck U. Local delivery of paclitaxel to inhibit restenosis during angioplasty of the leg. The New England journal of medicine. 2008; 358:689–699. [PubMed: 18272892]
5. Werk M, Langner S, Reinkensmeier B, Boettcher HF, Tepe G, Dietz U, Hosten N, Hamm B, Speck U, Ricke J. Inhibition of restenosis in femoropopliteal arteries: paclitaxel-coated versus uncoated balloon: femoral paclitaxel randomized pilot trial. Circulation. 2008; 118:1358–1365. [PubMed: 18779447]
6. Scheller B, Speck U, Abramjuk C, Bernhardt U, Bohm M, Nickenig G. Paclitaxel balloon coating, a novel method for prevention and therapy of restenosis. Circulation. 2004; 110:810–814. [PubMed: 15302790]
7. Scheller B, Hehrlein C, Bocksch W, Rutsch W, Haghi D, Dietz U, Bohm M, Speck U. Treatment of coronary in-stent restenosis with a paclitaxel-coated balloon catheter. N Engl J Med. 2006; 355:2113–2124. [PubMed: 17101615]

8. Granada JF, Milewski K, Zhao H, Stankus JJ, Tellez A, Aboodi MS, Kaluza GL, Krueger CG, Virmani R, Schwartz LB, Nikanorov A. Vascular response to zotarolimus-coated balloons in injured superficial femoral arteries of the familial hypercholesterolemic Swine. Circ Cardiovasc Interv. 2012; 4:447–455. [PubMed: 21953371]
9. Belkacemi A, Agostoni P, Nathoe HM, Voskuil M, Shao C, Van Belle E, Wildbergh T, Politi L, Doevendans PA, Sangiorgi GM, Stella PR. First results of the DEB-AMI (drug eluting balloon in acute ST-segment elevation myocardial infarction) trial: a multicenter randomized comparison of drug-eluting balloon plus bare-metal stent versus bare-metal stent versus drug-eluting stent in primary percutaneous coronary intervention with 6-month angiographic, intravascular, functional, and clinical outcomes. J Am Coll Cardiol. 2012; 59:2327–2337. [PubMed: 22503057]
10. Hamm, CW.; Cremers, B.; Moellmann, H.; Mobius-Winkler, S.; Zeymer, U.; Vrolix, M.; Schneider, S.; Dietz, U.; Bohm, M.; Scheller, B. Paclitaxel-Eluting PTCA-Balloon in Combination with the Coroflex Blue Stent vs the Sirolimus Coated Cypher Stent in the Treatment of Advanced Coronary Artery Disease. Paper presented at: American Heart Association Scientific Sessions; 2009; Orlando, FL.
11. Tzafriri AR, Vukmirovic N, Kolachalama VB, Astafieva I, Edelman ER. Lesion complexity determines arterial drug distribution after local drug delivery. J Control Release. 2010; 142:332–338. [PubMed: 19925836]
12. Tzafriri AR, Levin AD, Edelman ER. Diffusion-limited binding explains binary dose response for local arterial and tumour drug delivery. Cell Prolif. 2009; 42:348–363. [PubMed: 19438899]
13. Creel CJ, Lovich MA, Edelman ER. Arterial paclitaxel distribution and deposition. Circulation research. 2000; 86:879–884. [PubMed: 10785510]
14. Zhao HQ, Jayasinghe D, Hossainy S, Schwartz LB. A theoretical model to characterize the drug release behavior of drug-eluting stents with durable polymer matrix coating. J Biomed Mater Res A. 2012; 100:120–124. [PubMed: 21997889]
15. Hossainy S, Prabhu S. A mathematical model for predicting drug release from a biodurable drug-eluting stent coating. J Biomed Mater Res A. 2008; 87:487–493. [PubMed: 18186043]
16. Tepe G, Schmitmeier S, Speck U, Schnorr B, Kelsch B, Scheller B. Advances on drug-coated balloons. J Cardiovasc Surg (Torino). 2010; 51:125–143.
17. Speck U, Cremers B, Kelsch B, Biedermann M, Clever YP, Schaffner S, Mahnkopf D, Hanisch U, Bohm M, Scheller B. Do pharmacokinetics explain persistent restenosis inhibition by a single dose of paclitaxel? Circ Cardiovasc Interv. 2012; 5:392–400. [PubMed: 22619258]
18. Hwang CW, Wu D, Edelman ER. Impact of transport and drug properties on the local pharmacology of drug-eluting stents. Int J Cardiovasc Intervent. 2003; 5:7–12. [PubMed: 12623559]
19. Levin AD, Vukmirovic N, Hwang CW, Edelman ER. Specific binding to intracellular proteins determines arterial transport properties for rapamycin and paclitaxel. Proc Natl Acad Sci U S A. 2004; 101:9463–9467. [PubMed: 15197278]
20. Hwang CW, Edelman ER. Arterial ultrastructure influences transport of locally delivered drugs. Circ Res. 2002; 90:826–832. [PubMed: 11964377]
21. Levin AD, Jonas M, Hwang CW, Edelman ER. Local and systemic drug competition in drug-eluting stent tissue deposition properties. J Control Release. 2005; 109:236–243. [PubMed: 16289420]
22. Elmalak O, Lovich MA, Edelman E. Correlation of transarterial transport of various dextrans with their physicochemical properties. Biomaterials. 2000; 21:2263–2272. [PubMed: 11026632]
23. Baldwin AL, Wilson LM, Gradus-Pizlo I, Wilensky R, March K. Effect of atherosclerosis on transmural convection an arterial ultrastructure. Implications for local intravascular drug delivery. Arterioscler Thromb Vasc Biol. 1997; 17:3365–3375. [PubMed: 9437181]
24. Kolachalama VB, Levine EG, Edelman ER. Luminal flow amplifies stent-based drug deposition in arterial bifurcations. PLoS One. 2009; 4:e8105. [PubMed: 19956555]
25. Kolachalama VB, Tzafriri AR, Arifin DY, Edelman ER. Luminal flow patterns dictate arterial drug deposition in stent-based delivery. J Control Release. 2009; 133:24–30. [PubMed: 18926864]

Clinical perspective

Local drug delivery from endovascular balloons, investigated decades ago has been rejuvenated with the expectation that issues like thrombosis with drug-eluting stents (DES) and late lumen loss with bare metal stents could be avoided. Early failures of heparin-eluting catheters and balloons were attributed to poor retention of hydrophilic drugs, and indeed hydrophobic Paclitaxel is retained, as it associates with hydrophilic carriers to enhance transfer from blood to the artery wall and retention when dissociated. It remained unclear though whether Sirolimus derivatives such as Zotarolimus that are efficacious when released from DES, but may not use the same transport enhancing mechanisms as Paclitaxel could demonstrate comparable efficacy when coated on balloons. Our work is the first to describe the mechanisms of Zotarolimus-coated balloon (ZCB) therapy using an integrative approach coupling *in vivo* studies, bench-top experiments and computational modeling. Large bolus of balloon released Zotarolimus and its constituents transfer during inflation, some drug pervades the tissue and a fraction of the drug coating adheres to the tissue-lumen interface. The duration of balloon exposure to the tissue-lumen interface determines net drug uptake into tissue, where diffusion mediates transport into the arterial wall and reversible binding to tissue ultrastructural elements determines retention of Zotarolimus in an arterial bed dependent manner. Therefore, there is a theoretical basis for balloon delivery of Zotarolimus to the arterial wall to be clinically efficacious, and that optimization of ZCB therapy may rely on tailoring of balloon coating, drug release kinetics, and inflation time to the arterial target.

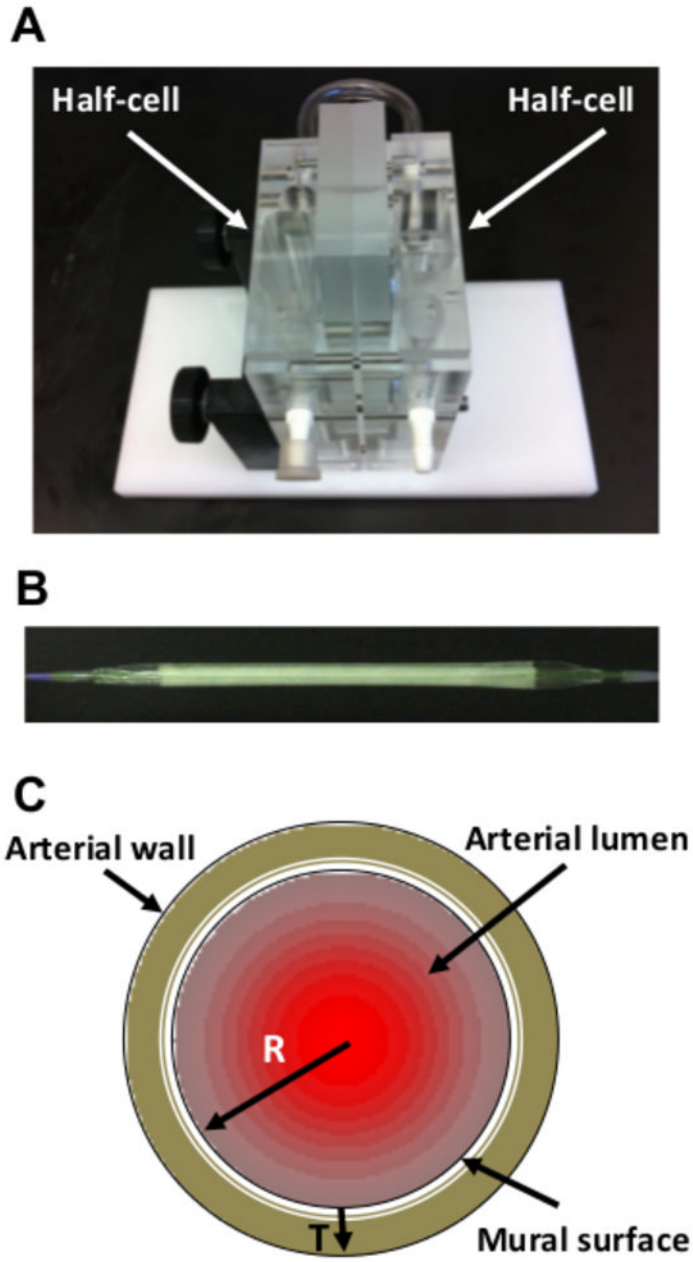

Figure 1.

Experimental apparatus and computational model setup. (A) A custom modified, acrylic vertical diffusion chamber was used for estimating transmural drug uptake within the tissue. Tissue was affixed within the insert using a series of pins surrounding the opening. (B) A representative 6×40 mm Zotarolimus-coated balloon. (C) Schematic of the computational model used for the study, with balloon fully expanded and presumably transferring drug to the mural surface. R is the lumen radius and T denotes the tissue thickness.

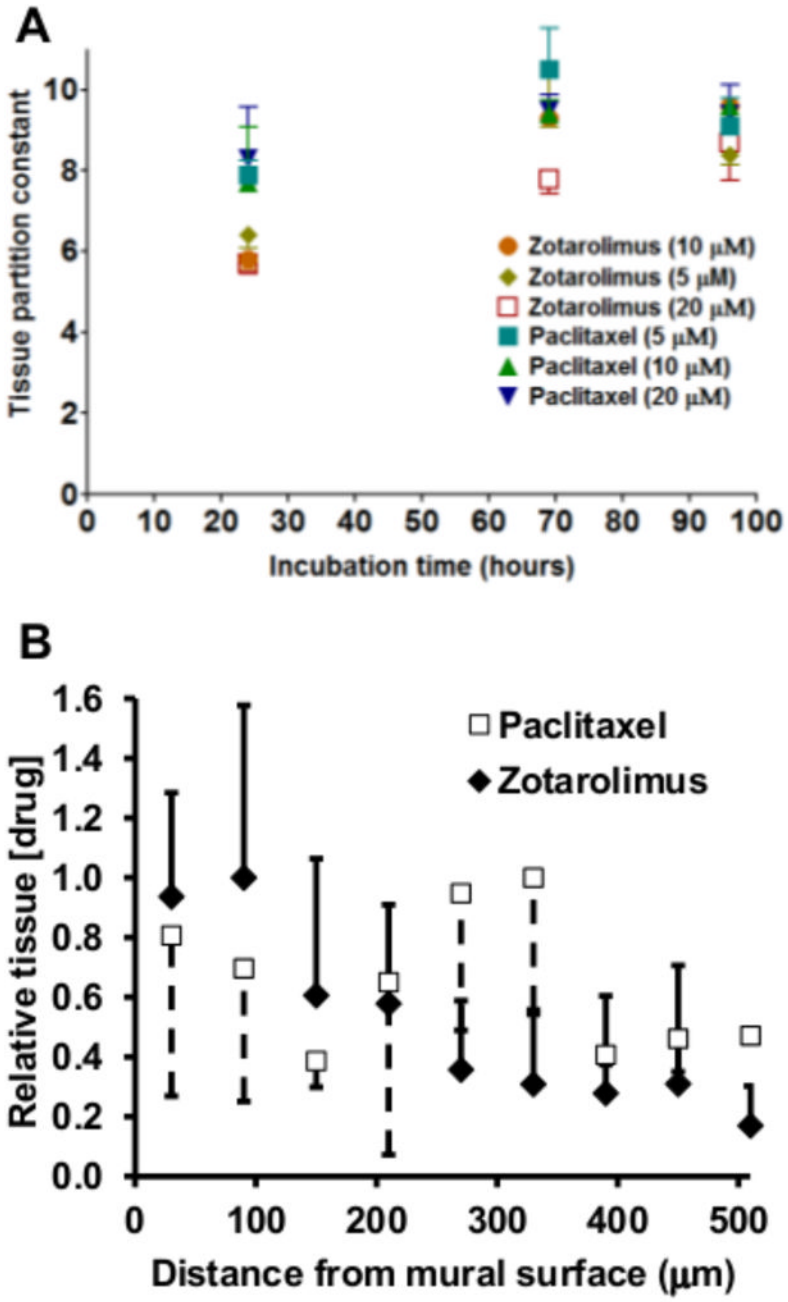

Figure 2.

Bench-top estimation of drug transport parameters. (A) Net tissue partition constants of Zotarolimus and Paclitaxel as a function of time at three bath concentrations. Curve fitting of experimental results at 69 hrs provided estimates of equilibrium binding parameters (K_d & B_M) for both drugs. (B) Normalized transmural distributions of Zotarolimus and Paclitaxel reveal spatial gradients of both drugs across the arterial wall. Three consecutive transmural slices, each cryosectioned at 20 μm thicknesses were grouped together to compute the mean concentration and plotted as a function of the average distance of the grouped slices from the transmural location. Plotted drug concentrations are normalized with the highest estimated value for each drug.

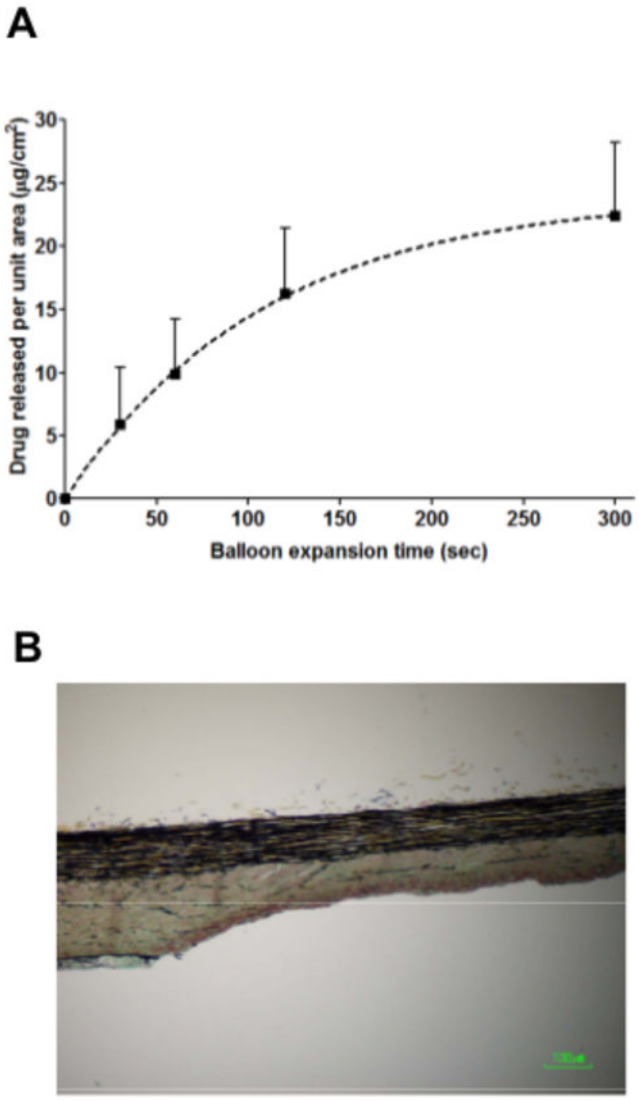

Figure 3.

(A) Zotarolimus release normalized to balloon surface area during balloon expansion. ZCBs were fully expanded and immersed in baths of porcine blood at different times and Zotarolimus content per unit area of each balloon was quantified. ZCB kinetics exhibited a first order release profile with constants A_1 and k_1 (Equation 4) estimated as 24 $\mu g/cm^2$ and 0.009221 s^{-1}, respectively ($R^2 = 0.9999$). (B) Microphotograph showing post deployed state of the arterial wall with the balloon coating constituents comprising Zotarolimus adhered to the mural surface.

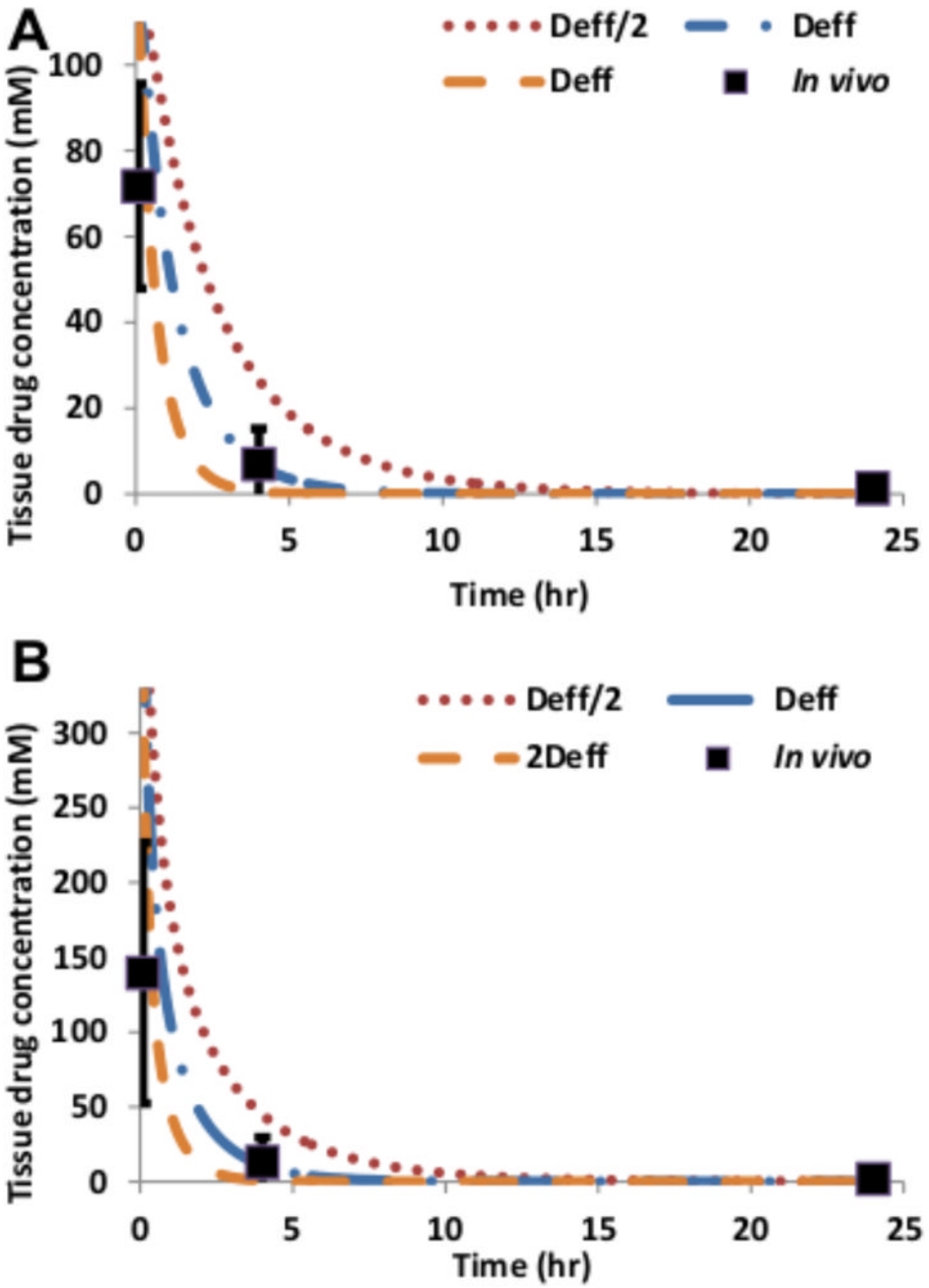

Figure 4.

Temporally varying computational predictions correlate with *in vivo* estimates of Zotarolimus uptake for both inflation times (30 s (A) & 180 s (B)). Here, concentration was estimated by calculating total drug per unit mass of arterial tissue.

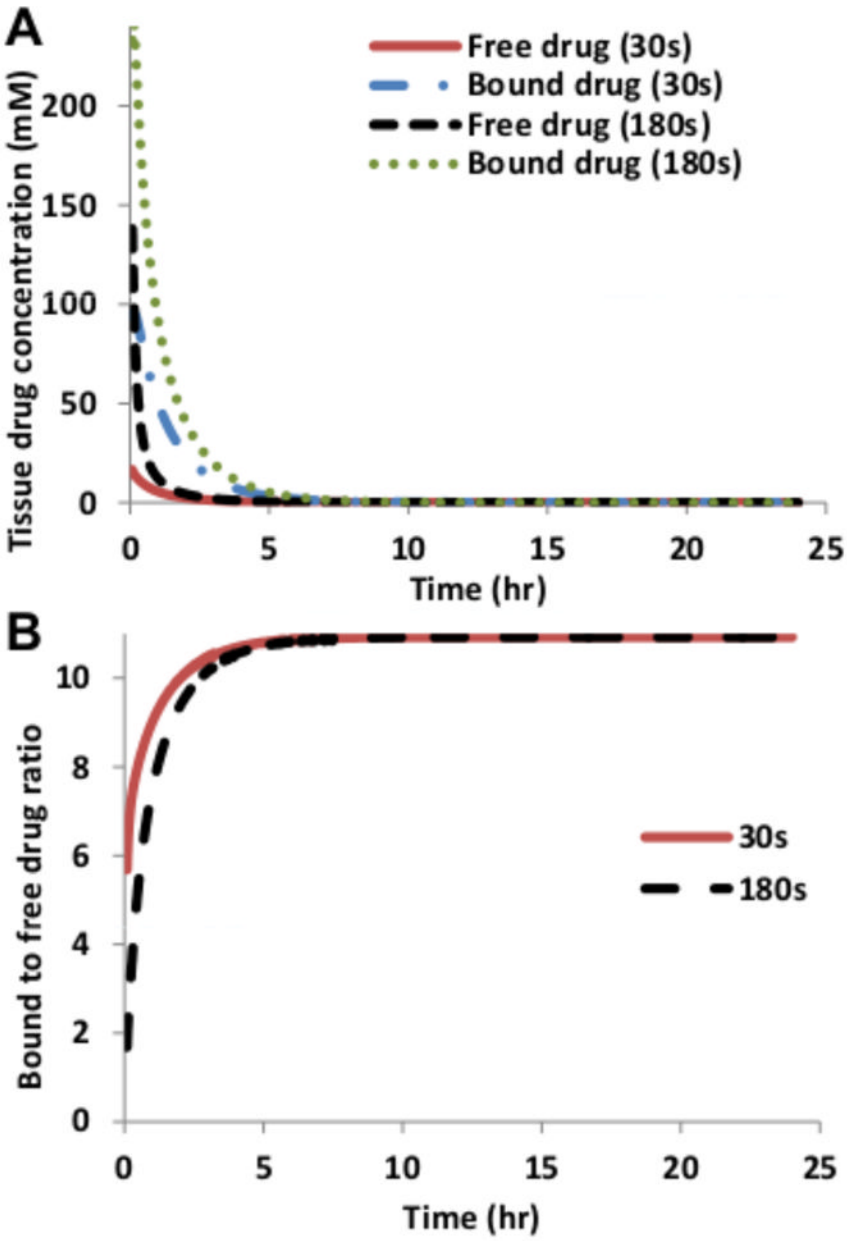

Figure 5.

(A) Temporal distribution of bound and unbound Zotarolimus elucidates the role of reversible binding within arterial tissue (D_T = 17.12 $\mu m^2/s$). (B) Ratio of bound to unbound drug increases over time and reaches a steady state within ~5 hrs after balloon inflation.

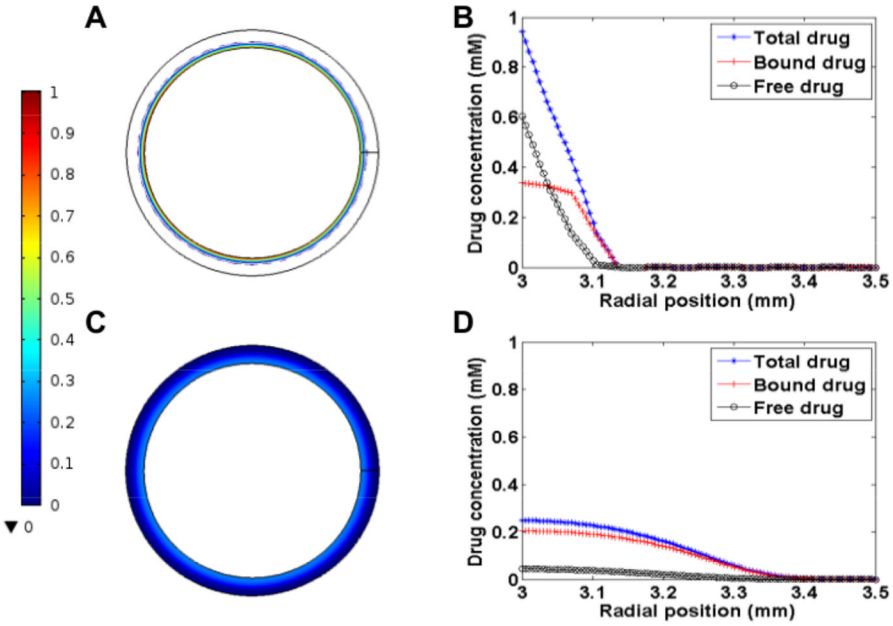

Figure 6.

Computational predictions of Zotarolimus arterial distribution. (A) Total drug concentration after exposure to 30 s balloon inflation is maximal at the mural surface and declines up to a penetration depth of ~130 μm (B). By 5 min after the onset of balloon inflation (C), Zotarolimus is distributed across the arterial wall with a peak that is ~25% of that of the peak at 30 s. Due to diffusive clearance of free Zotarolimus at the luminal and adventitial aspects, drug is predominantly bound by 5 min (D).